Regulation on mechanical properties of spherically cellular fruits under osmotic stress

Shaobao Liu [a,b,c,#], Haiqian Yang [d,e,#], Zitong Bian [d,e], Ru Tao [b,c], Xin Chen [c,d,e], Tian Jian Lu [a,c,d,*]

[a] State Key Laboratory of Mechanics and Control of Mechanical Structures, Nanjing University of Aeronautics and Astronautics, Nanjing 210016, PR China
[b] The Key Laboratory of Biomedical Information Engineering of Ministry of Education, School of Life Science and Technology, Xi'an Jiaotong University, Shaanxi 710049, PR China
[c] Bioinspired Engineering & Biomechanics Center (BEBC), Xi'an Jiaotong University, Xi'an 710049, PR China
[d] MOE Key Laboratory for Multifunctional Materials and Structures, Xi'an Jiaotong University, Xi'an 710049, PR China
[e] State Key Laboratory for Strength and Vibration of Mechanical Structures, School of Aerospace, Xi'an Jiaotong University, Xi'an 710049, PR China

A R T I C L E   I N F O

A B S T R A C T

The texture of fruits is closely related to their mechanical properties (*e.g.*, elastic modulus), which is largely influenced by the osmotic stress. As known to all, the turgor pressure changes under osmotic stress. However, it is unclear how osmotic stress quantitatively changes the turgor pressure and deforms the cells, which further affects the mechanical properties of fruits. In the current study, combining the van't Hoff theory of osmotic pressure with the self-consistent method, we developed a cross-scale theoretical model by considering the osmotic equilibrium, mechanical balance and substance conservation. We found that increasing the external osmotic stress changes the osmotic equilibrium, decreases the turgor pressure, shrinks the cells, enlarges the intercellular space, and softens the fruit tissue. The estimated Young's modulus under osmotic stress agrees with the experimental results.

© 2019 Elsevier Ltd. All rights reserved.

1. Introduction

The mechanical properties are important indicators of the texture (*e.g.*, crumbly, creamy, render, soft or hard) of fruits (Deng et al., 2005; Piotrowski et al., 2014). Fruits typically have hierarchical structure with varying mechanical properties and texture but similar components (Fig. 1). The macroscale mechanical properties of stored fruits are closely determined by the environmental factors (*e.g.*, osmotic stress), the microscale structure (*e.g.*, volume fraction of intercellular space, size of the cells and thickness of the cell walls), and the microscale mechanical properties (*e.g.*, cell-wall Young's modulus and turgor pressure) (Aguilera, 2005; Gibson, 2012). It is therefore necessary to make it clear how to bridge between the macroscale mechanical properties of fruits and the osmotic stress, the hierarchical structure, and the cell-level mechanical properties.

---

* Corresponding author at: State Key Laboratory of Mechanics and Control of Mechanical Structures, Nanjing University of Aeronautics and Astronautics, Nanjing 210016, PR China.
  E-mail address: tjlu@nuaa.edu.cn (T.J. Lu).
# Co-first authors: They contributed equally to this work.

There exist extensive studies attempting to relate the macroscale mechanical properties of fruits with their microscale mechanical and structural parameters. For example, the influence of turgor pressure (osmotic stress dependent) on the geometrical structure of cells and the mechanical properties of potato and apple tissue was experimentally studied (Falk, 1958; Lin and Pitt, 2010; Oey et al., 2007). Theoretical models were also developed to reveal the effect of turgor pressure and cell-wall mechanical properties on the Young's modulus of tissue by treating the potato tissue as a matrix of liquid-filled spherical cells (Nilsson, 1958) or hexagonal cells (Singh et al., 2013, 2014; Zhu and Melrose, 2003). Commonly, the input variable in the mechanical models of fruits is the turgor pressure, rather than the osmotic stress. Thus, it is important to make it clear how osmotic stress quantitatively affects turgor pressure in cells and how it deforms the cells, which further affects the mechanical properties of fruits.

In the present study, we propose a theoretical framework for relating the macroscale mechanical properties of fruits to the osmotic stress, the hierarchical structure and microscale mechanical properties. We have neglected viscoelasticity and poroelasticity (the coupling of water flow and deformation). This is because the mechanical properties (elasticity, viscoelasticity and poroelasticity) of liquid-filled porous media can be decoupled through controlling properly the loading rate (Hu and Suo, 2012). Thus, we focus on the physical mechanisms behind the softening process (*i.e.*, elasticity changing) of fruits under osmotic stress. First, by considering the cell as a thin-walled spherical shell and combining the osmotic equilibrium, the substance conservation, the constitutive law of cell wall and the mechanical balance, we obtain the turgor pressure and the deformation of cells under osmotic stress. Second, based on the spherical composite element model (Hashin, 1962; Nemat-Nasser and Hori (1993)), we determine the equivalent bulk modulus and shear modulus of a cell. Finally, employing the self-consistent method (Hill, 1963; 1965), the equivalent Young's modulus and Poisson ratio of tissue are calculated.

2. Materials and methods

2.1. Microstructure observation of fruit tissue

The basic microstructures of plant tissue are honey-comb-like cells (*e.g.*, woods), closed-cell, liquid-filled parenchyma cells (*e.g.*, apples and potatoes) and composites of these two (Gibson, 2012). In the present study, we focus on liquid-filled spherically cellular parenchyma fruits having the closed cells, such as apple, gandaria, date, kiwifruit, tomato, potato and etc. Fresh fruits, including apple, gandaria, kiwifruit and tomato, were bought from local markets (Xi'an, Shaanxi, China) for microstructure observation. The microstructures of sliced fruits were then observed under ultra-well deep microscope (KEYENCE VHX-5000, Japan). No obvious difference in microstructure of apple tissue was observed from mesocarp to exocarp (Fig. 1(a)). However, the size of cells decreases rapidly in the part of apple immediately adjacent to its skin. Denote this part as the outer layer of apple which covers a tissue range of about 1000 μm near the edge (skin) and denote the inner part (the remaining part) as the inner layer. Cell size measurements for apple indicates that the average cell diameter
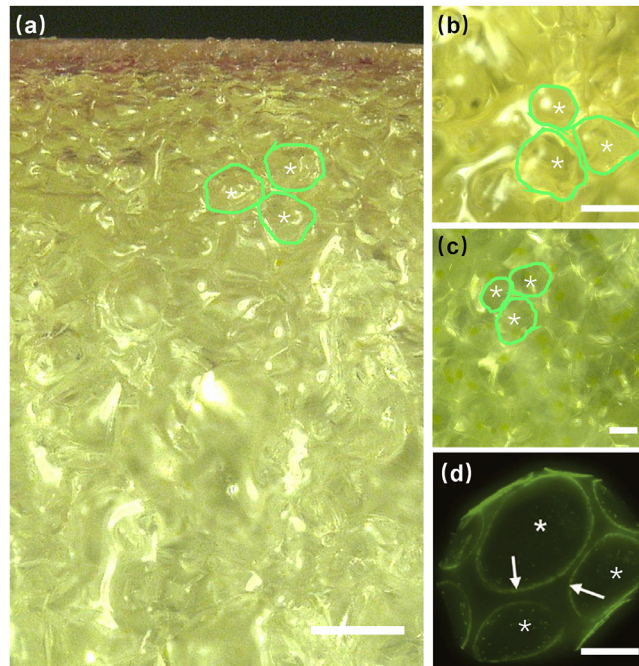
Fig. 1. Observations of fruit cells in a digital microscope. (a) Apple; (b) Gandaria; (c) Kiwifruit; (d) Tomato with former edge of adhesion planes (arrows) (Ordazortiz et al., 2009). Scale bar (a) 200 μm; (b-d) 100 μm.
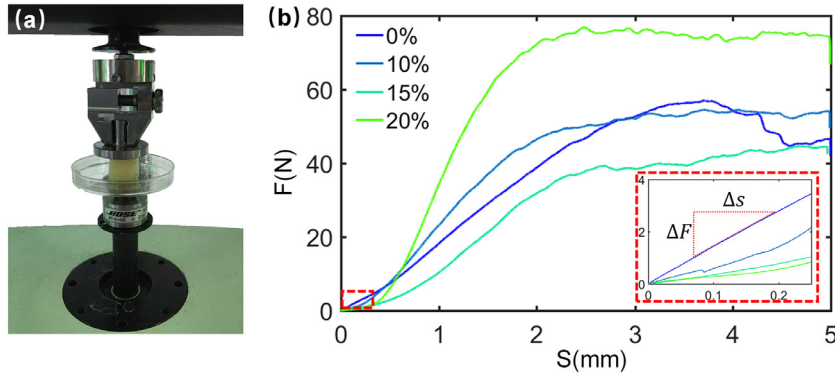
Fig. 2. Compression test of apple tissue. (a) The mechanics test system (Bose Electricforce 3220); (b) Force-displacement curves for the samples soaked in 0%, 10%, 15% and 20% sucrose solution.

of the inner layer (which is approximately uniform) is ~164 μm, and the average cell diameter of cells adjacent to cuticle is ~39 μm. A closer look of the inner tissue revealed that the cells are not pressed together but exhibit intercellular spaces. Fruit tissue consists of intercellular matrix and inclusions of cells with arbitrary orientation and different sizes. The cells are almost homogeneously distributed and well-separated in the intercellular matrix (Fig. 1(b-d)). The volume fraction of cells is high, varying in the range of 0.6–0.8. Thus, the parenchymal fruits (*i.e.*, apple, gandaria, kiwifruit and tomato) are made up of tissues having similar microstructures (spherical cells with thin cell wall). Consequently, in the remaining sections of this study, we just choose apple as the template for experimental measurements and theoretical calculations.

2.2. Measuring the Young's modulus of apple tissue under osmotic stress

As a representative fruit with liquid-filled parenchyma cells, apples are popular, favorited, and grown widely all over the world. Consequently, in the current study, apples are taken as the example to study their mechanical properties under osmotic stress. Fresh apples were held at 4°C in controlled atmosphere storage until experimentation. To exclude the effect of individual difference, block samples (1.5 × 1.5 × 1.5 cm) were cut from one apple. Four nominally identical samples were then soaked in 1 L (sufficiently large to keep constant concentration) sucrose solutions with different concentrations (mass fraction 0%, 10%, 15%, 20%) for 24 h (referred to 30–36 h (Lin and Pitt, 2010)) at room temperature. To prevent tissue degradation during soaking, the sucrose solutions were buffered with 0.02 M K_2HPO_4 and 0.02 M KH_2PO_4 (Lin and Pitt, 2010).

When the loading rate is fast enough both the viscoelastic relaxation and poroelastic relaxation have not yet started, so that the material could be considered as linear elastic (Hu and Suo, 2012). In the present study, all the test samples were compressed in the solutions by a displacement of 5 mm under a mechanics test system (Bose Electricforce 3220) (Fig. 2(a)). The time scale of poroelastic relaxation (τ_D) is related to the diffusion coefficient (*D*) and characteristic length (*L*), *i.e.*, $\tau_D \sim \frac{L^2}{D}$. For the material of apple tissue, the diffusion coefficient of is on the order of $\sim 10^{-11}$ m^2/s (Hou et al., 2005). The characteristic length of the experiment is on the order of 10^{-2} m. The poroelastic relaxation time is thus on the order of hours. A typical value of the viscoelastic relaxation of cells is in $\sim 10–10^2$ s (Aregawi et al., 2013). In our case of apple tissue, the loading rate is 0.15 mm/s (much faster than 2 μm/s of indention (Hu et al., 2011) and the displacement is 0.25 mm, which are sufficiently fast such that both the viscoelastic relaxation and poroelastic relaxation have not yet started. Consequently, in the current study, the behaviors of viscoelasticity and poroelasticity could be neglected. During the experiments, with the initial compressive force prescribed as 0.1 N (excluding the initially deformation from first contact between the puncher and the test sample till full contact), force-displacement curves for each sample were recorded (Fig. 2(b)). Within the regime of small displacement (less than 0.25 mm), the deformation may be taken as linear so that the Young's modulus (E_{tissue}) of apple tissue was calculated as

$$E_{tissue} = \frac{1}{L}\frac{\Delta F}{\Delta S} \tag{1}$$

where $L = 1.5$ cm is the size of the sample block, ΔF is the increment of force and ΔS is the increment of displacement, as shown in Fig. 2(b).

2.3. Cross-scale mechanical models of fruits

The fruit tissue is composed of intercellular materials and cells with different sizes, the cell being typically a permeable sphere filled with cytoplasm (Fig. 3). As the cells inevitably deform under osmotic stress, we first estimated the turgor pressure and deformation of the cell as functions of the osmotic stress. Further, we calculate the equivalent elastic properties of the deformed fruit tissue.
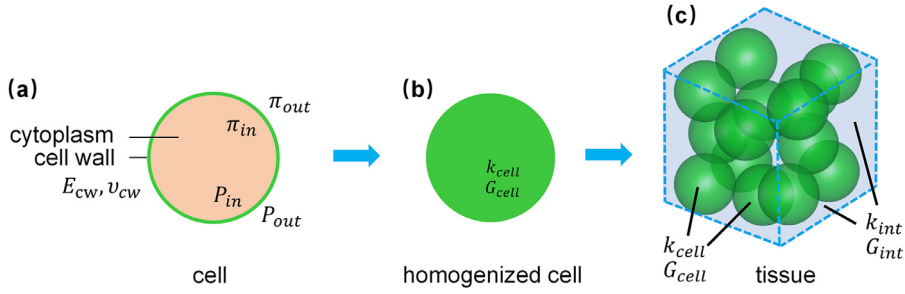
Fig. 3. Homogenization model of spherically cellular fruit. (a) Fruit cell with cell wall. P_{in} is the water static pressure inside the cell, π_{in} is the osmotic pressure inside the cell, P_{out} is the water static pressure outside the cell and π_{out} is the osmotic pressure outside the cell. (b) Homogenized cell; (c) tissue with cubic closest-packed spherical cells. The cells are spheres with k_{cell} and G_{cell}. Intercellular medium, which is a composite of cellulose and pectin, is considered as an elastic material with bulk modulus k_{int} and shear modulus G_{int}.

2.3.1. Modeling the turgor pressure and deformation of fruit cell under osmotic stress

To fully understand the influence of osmotic stress on the deformation of cells and changes in cellular turgor pressure, we coupled the osmotic equilibrium of water with the mechanical equilibrium of cell wall (Fig. 3(a)).

2.3.1.1. Osmotic equilibrium. Jacobus van't Hoff, who got the Nobel Prize in 1901, proposed the theory of osmotic equilibrium. When two solutions with different concentration separated by a semi permeable membrane (*e.g.* cell membrane), the membrane allows water but not solute (*e.g.*, sugar) to pass through it. The concentration difference forces the water into the solution of higher concentration, which exerts an extra pressure on the membrane. The extra pressure is defined as osmotic pressure and can be estimated as $\Delta\Pi = \Delta cRT$, where $\Delta c = c_i - c_o$ is the concentration difference of sugar, c_i is the concentration inside the cell, c_o is the concentration outside the cell, R is the universal gas constant, and T is the temperature. Considering the equilibrium state of a saturated cell, the turgor pressure (ΔP, the force bearing on cell wall) of the cell equals to the osmotic pressure difference ($\Delta\Pi$), namely:

$$\Delta P = \Delta\Pi \tag{2}$$

The turgor pressure (ΔP) equals to the hydrostatic pressure difference: $\Delta P = P_i - P_o$, where P_i and P_o are the hydrostatic pressure inside and outside the cell, respectively. The osmotic pressure is $\Delta\Pi = \Pi_i - \Pi_o$, Π_i being the osmotic pressure inside the cell and Π_o the osmotic pressure outside the cell.

2.3.1.2. Mechanical balance. Cell wall is regarded as isotropic, thin and uniform in thickness. Consider a hypothetical section that divides the spherical cell into two hemi-spheres. Mechanical balance then dictates that $\sigma = \Delta P(r-t)/2t$. When the cell wall is deformed, it experiences a strain of $\varepsilon_{xx} = \varepsilon_{yy} = \frac{\sigma_{cw}(1-v_{cw})}{E_{cw}}$ so that its current surface area is $A = L_x(1+\varepsilon_{xx})L_y(1+\varepsilon_{yy})$. Combining these two equations and assuming an initial stress σ_0 on the cell wall, we get $\sigma = \frac{E_{cw}}{2(1-v_{cw})}\left(\frac{A}{A_0}-1\right) + \sigma_0$. Together with the mechanical balance and the initial condition, $\Delta P = \Delta P_0$ and $r = r_0$, we arrive at:

$$\Delta P = \frac{2t}{r-t}\frac{E_{cw}}{2(1-v_{cw})}\left(\frac{r^2}{r_0^2}-1\right) + \Delta P_0 \tag{3}$$

For simplicity, assuming the total volume of the cell wall is constant, we have:

$$r^3 - (r-t)^3 = r_0^3 - (r_0-t_0)^3 \tag{4}$$

In the above equations, σ is the stress of cell wall, σ_0 is the initial stress of cell wall, r is the current radius of cell, r_0 is the radius of cell at initial state, t is the current thickness of cell wall, t_0 is thickness of cell wall at initial state, ΔP_0 is the turgor pressure at initial state, and E_{cw} is the cell-wall Young's modulus.

2.3.1.3. Substance conservation. Water flow, passive diffusion and active transport are the three main mass exchange out and in cells (Jiang and Sun, 2013). For simplicity, we only consider the water flow when the osmotic stress is just induced by one solute of macromolecules (*e.g.*, sugar). Because the macromolecular cannot travel through the membrane of cell, the amount of macromolecule in cell is constant, yielding:

$$c_{i0}V_{cell0} = c_iV_{cell} \tag{5}$$

where $V_{cell} = \frac{4}{3}\pi r^3$ is the current volume of cell, V_{cell0} is the volume of cell at initial state, c_{i0} is the concentration inside cell at the initial state.

The concentration inside cell (c_i), the turgor pressure (ΔP), the radius of cell (r), and thickness of cell wall (t) are determined by solving Eqs. (1)–(5).

2.3.2. Equivalent elastic properties of fruit tissue

2.3.2.1. Equivalent bulk modulus and shear modulus of solid spherical cell. To estimate the equivalent elastic properties of fruit tissue using the popular homogenization method (Fig. 3(a) & (b)), the equivalent elastic properties of the inclusion (*i.e.*, the cells) have to be calculated first. Due to the semi permeability of cell membrane, water can travel freely through the membrane and the turgor pressure inside cell ΔP is controlled by osmotic pressure difference $\Delta \Pi$ so that the effect of the intercellular part can be treated as a constant turgor pressure when the cell is subjected to infinitely small load. For a shell structure having constant turgor pressure, its equivalent bulk modulus and equivalent shear modulus can be estimated using the classical models developed initially for estimating the overall properties of heterogeneous materials, such as the models of Hashin (1962), Nemat-Nasser and Hori (1993), as:

$$\frac{k_{cell}}{k_{cw}} = (1 - \phi_{cell}) \frac{2 - 4v_{cw}}{\phi_{cell}(1 + v_{cw}) + 2 - 4v_{cw}} \tag{6}$$

$$\frac{G_{cell}}{G_{cw}} = (1 - \phi_{cell}) \frac{7 - 5v_{cw}}{15(1 - v_{cw})} \tag{7}$$

where k_{cw} is the bulk modulus of the cell wall, G_{cw} is the shear modulus of the cell wall, v_{cw} is the Poisson ratio of cell wall, and $\phi_{cell} = (\frac{r-t}{r})^3$ is the volume ratio of the cytoplasm to the cell.

2.3.2.2. Equivalent bulk modulus and shear modulus of tissue. Eshelby (1957) famously estimated the equivalent elastic properties of a matrix embedded with an ellipsoidal inclusion by solving the elastic field. When the inclusions are closer, the interaction between inclusions should be involved. Mori and Tanaka (1973) proposed an approach to calculate the average strain of the inclusions by modifying the far field strain. However, the Mori-Tanaka method is not appropriate when the volume fraction of the inclusions is high. Based on the Hashin and Shtrikman (1962) variational principle in terms of phase properties and their volume fractions, Hill (1965), Budiansky (1965) and Kroner (1978) proposed the self-consistent method by treating the matrix phases as homogenized ones.

Among these methods, the self-consistent method is useful when the distribution of the inclusions is unspecified and the volume fraction of inclusions is relatively high. Thus, the self-consistent method is more suitable for evaluating the equivalent mechanical properties of tissue with high volume fraction of cell inclusions. Note that the statistical information about cell distribution is adopted in the self-consistent method.

For simplicity, the tissue is assumed to have a matrix in which spherical inclusions of cells are embedded (Fig. 3(c)). Both the intercellular matrix and the cells are considered as isotropic, and the distribution of inclusions is taken as homogeneous and well-separated. According to the self-consistent method, the equivalent bulk modulus (k_{tissue}) and equivalent shear modulus (G_{tissue}) of tissue are obtained by solving the following equations (Hill, 1963; 1965):

$$k_{tissue} = k_{int} + \frac{\left(1 - \phi_{tissue}{}^{\lambda}\right)(k_{cell} - k_{int})(3k_{tissue} + 4G_{tissue})}{3k_{cell} + 4G_{tissue}} \tag{8}$$

$$G_{tissue} = G_{int} + \frac{5\left(1 - \phi_{tissue}{}^{\lambda}\right)G_{tissue}(G_{cell} - G_{int})(3k_{tissue} + 4G_{tissue})}{3k_{tissue}(3G_{tissue} + 2G_{cell}) + 4G_{tissue}(2G_{tissue} + 3G_{cell})} \tag{9}$$

where k_{int} and G_{int} are separately the bulk modulus and shear modulus of intercellular material. $\phi_{tissue} = 1 - \frac{V_{cells}}{V_{tissue}}$ is the volume fraction of intercellular space of tissue. V_{tissue} is the volume of tissue and V_{cells} is the overall volume of all cells in the tissue. Note that V_{tissue} changes little under osmotic stress, as verified in the experiment. Combined with Eq. (5) and eliminating V_{cells} and V_{tissue}, the volume fraction can be rewritten as $\phi_{tissue} = 1 - \frac{c_{i0}}{c_i}(1 - \phi_{tissue0})$.

In the classical self-consistent method, $\lambda = 1$, which suggests that the impact of inclusions on the equivalent modulus of tissue is linear. However, when the volume fraction of inclusions becomes sufficiently high, the self-consistent method becomes inaccurate, a typical example of which is the face-centered cubic volume element (Fig. S1). This deviation is caused by the nonlinear interaction between inclusions and thus the self-consistent method should be modified. Inspired by Dixon et al. (2018), who introduced power law to demonstrate the equivalent modulus of plant tissue, we assume that the value of λ could be modified to demonstrate the nonlinear interaction between inclusions. The distribution of inclusions affects the value of λ. For face-centered cubic inclusions, $\lambda = 0.72$ presents the best fit for finite element results, as illustrated in Fig. S1.

3. Results and discussion

3.1. Effects of cell-wall mechanical properties on elastic modulus of a single cell

Using the baseline parameters listed in Table 1, we estimated the equivalent bulk modulus of a single cell as 2.0 MPa, and the equivalent shear modulus as 1.2 MPa. Further, we estimated the equivalent Young's modulus of a single cell as 2.0 MPa, which is somewhat larger than the experimental value (0.21 – 1.05 MPa) (Cárdenas-Pérez et al., 2016). Nonetheless, the

Table 1
Symbols and parameters of fruits.

| Symbols	Physical properties	Value	Baseline
P	Turgor pressure[†]	0.3–1 MPa (typical turgor pressure in plants) (Wei and Lintilhac, 2007)	2 MPa
		0.8–1.4 MPa (Arabidopsis) (Forouzesh et al., 2013)	
		1–10 MPa (leaf petiole,varied in the model) (Faisal et al., 2010)	
		Maximum value of 5 MPa (Guard cell of Huperzia prolifera, Nephrolepis exaltata, Tradescantia virginiana and Triticum aestivum) (Franks and Farquhar, 2007)	
		0.363 MPa (tomato) (Wang et al., 2004)	
E_{cw}	Young's modulus of cell wall[†]	0.2–6 GPa (potato, micro-penetration test) (Hiller et al., 1996)	0.16 GPa
		Maximum value of 130 GPa (potato, back calculated from tissue properties) (Hepworth and Bruce, 2000)	
		0.5–0.6 GPa (potato, estimated from the cell dimensions studied by Hepworth and Bruce et al. (Hepworth and Bruce, 2000)) (Gibson, 2012)	
		2.1 – 2.5 Gpa (2-week-old tomato) (Wang et al., 2004)	
v_{cw}	Poisson ratio of cell wall[†]	0.3–0.49 (potato) (Poisson ratio has little influence on back calculated cell-wall modulus from tissue) (Hiller et al., 1996)	0.33
		Taken to be 0.33 (parenchyma, i.e. potato) (Nilsson, 1958)	
		0.3–0.5 (tomato, taken in simulation) (Wang et al., 2004)	
v_{int}	Poisson ratio of intercellular material	Assumed	0.33
E_{int}	Young's modulus of intercellular material	6–100 kPa (calcium hydrogels derived from 1, 2 and 4% solutions of apple pectin) (Markov et al., 2017)	0.1 MPa
t	Thickness of cell wall[†]	0.1–3 μm (potato) (Hiller et al., 1996)	1 μm
		0.5–1.5 μm (potato) (Hepworth and Bruce, 2000)	
		~1 μm (total cell wall thickness of plants) (Gibson, 2012)	
		126 nm (tomato) (Wang et al., 2004)	
r	Radius of cell	19–82 μm (from cuticle to the inner layer; measured from Fig. 1)	80 μm
		~100 μm (apple and potato) (Gibson, 2012)	
$\phi_{tissue0}$	Initial volume fraction of intercellular space	0.2–0.25 (Pippin apple, gas spaces) (Bomben, 1982)	0.26
		0.26 (apple fruit peduncles, void spaces, assumed to be closest-packed spheres) (Horbens et al., 2015)	
c_{cell}	Concentration of sucrose solution inside cells	$\frac{P}{RT}$	807 mol/m^3

[†] Apple, tomato, potato are mostly made up of parenchyma tissue that stores sugar and have similar microstructures (Gibson, 2012). Tomato and potato have been extensively investigated and have more existing physical properties available. The physical properties of tomato and potato can be taken as references.
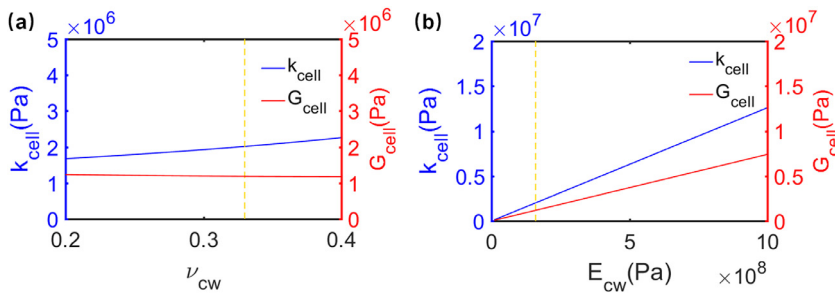
Fig. 4. Effect of elasticity properties of cell wall on bulk modulus (k_{cell}) and shear modulus (G_{cell}) of a single cell. (a) The effect of Poisson ratio (v_{cw}) of cell wall; (b) the effect of Young's modulus (E_{cw}) of cell wall. Yellow dash line represents the baseline of parameters. Solid lines represent the theoretical results.

estimated Young's modulus of apple cells is reasonable if taking into consideration that the Young's modulus of isolated apple cell is smaller than that in *vivo*, because the cell wall is partially damaged during the isolating process.

The effects of the Young's modulus and Poisson ratio of cell wall on the bulk modulus (k_{cell}) and shear modulus (G_{cell}) of a single cell were presented in Fig. 4. The bulk modulus (k_{cell}) and shear modulus (G_{cell}) of a single cell increase little as the Poisson ratio of cell wall is increased (Fig. 4(a)). The bulk modulus (k_{cell}) and shear modulus (G_{cell}) of a single cell increase obviously with the Young's modulus of cell wall (Fig. 4(b)). This is because, according to the rule of mixture (Liu, 1997; Wang et al., 2017), the equivalent modulus of the whole composite (apple cell) increases with the Young's modulus of one phase in the composite (cell wall).
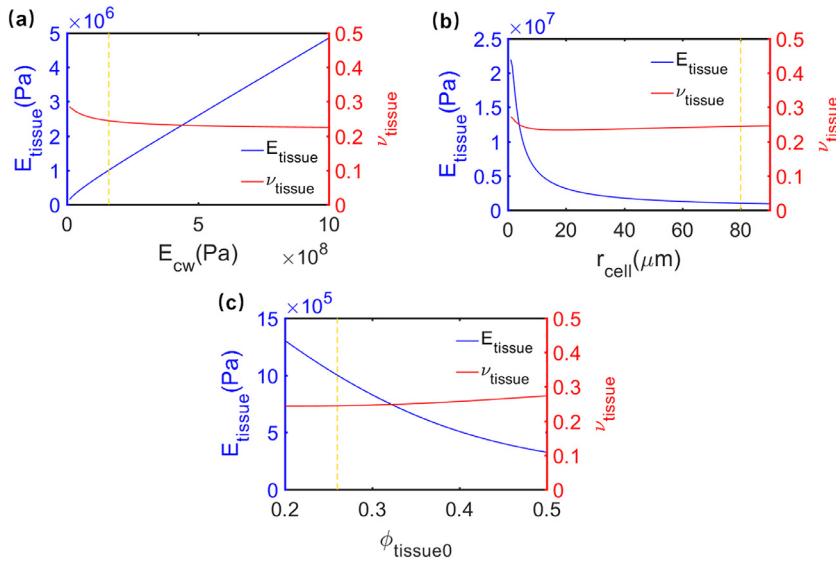
Fig. 5. The effect of elasticity properties of cell wall and structural properties of cells and tissue on elastic properties of tissue. (a) The effect of elastic properties (E_{cw}) of cell wall; (b) The effect of initial volume fraction of intercellular space ($\phi_{tissue0}$) in apple tissue; (c) The effect of cell radius (r_{cell}). Solid lines represent the theoretical results.

3.2. Effects of cell-wall mechanical properties and structure parameters of cells and tissue on mechanical properties of tissue

By using the baseline parameters of Table 1, the equivalent Young's modulus of tissue (cell diameter $\sim$160 μm) was calculated as 1.0 MPa, which falls in the range of existing experimental value (0.31 $\sim$ 5.8 MPa) (Cárdenas-Pérez et al., 2016; 2017; Lin and Pitt, 2010; Oey et al., 2007). Correspondingly, the equivalent Poisson ratio of tissue was calculated as 0.24, which is comparable to the existing value for cellulose in plant ($\sim$0.3) (Faisal et al., 2010). The influence of cell-wall Young's modulus (E_{cw}), volume fraction of intercellular space ($\phi_{tissue0}$) and radius of cell (r_{cell}) on the Young's modulus (E_{tissue}) and Poisson ratio (ν_{tissue}) of tissue was presented in Fig. 5. The Young's modulus of tissue (E_{tissue}) increases with increasing Young's modulus of cell wall (E_{cw}) (Fig. 5(a)) and decreases with increasing cell radius (r_{cell}) (Fig. 5(b)), consistent with existing studies (Gibson, 2012; Konstankiewicz et al., 2001; Nilsson, 1958). According to the rule of mixture (Liu, 1997; Wang et al., 2017), the whole composite (apple tissue) stiffens with the increase of Young's modulus of one phase (apple cell), when reducing the cell radius or increasing the Young's modulus of cell.

Previous models treated apple cells as densely packed with no intercellular space, but obvious void space was found on the micrograph of fruit tissues (Oey et al., 2007) (Fig. 1(c)) and also some intercellular spaces existed among cells (Ordazortiz et al., 2009). Taking the intercellular spaces into account, we found that the Young's modulus of tissue (E_{tissue}) decreases as the initial volume fraction of intercellular space ($\phi_{tissue0}$) is increased (Fig. 5(c)). That is because, according to the rule of mixture (Liu, 1997; Wang et al., 2017), the increase of volume fraction of soft phase (intercellular materials) softens the whole composite (apple tissue).

Comparing the proposed model to others, with baseline parameters in Table 1, the normalized Young's modulus of tissue $\frac{rE_{tissue}}{tE_{cw}}$ is 0.5 in the proposed model, which is smaller than 3.96 in Nilsson model (Nilsson, 1958) and 2.19 in Gibson model (Gibson, 2012). That is because, compared to the proposed model (random distribution and interaction of cells) the Nilsson model had regular arranged cells and Gibson model ignored the interaction between cells. Thus the results above are reasonable.

3.3. Equivalent Young's modulus and Poison ratio of apple tissue under osmotic stress

The change of external solution concentration (*i.e.*, osmotic stress) mainly influences the mechanical properties (Young's modulus and Poison ratio) of apple tissue from two aspects. On the one hand, the water loss from cells results in the decrease of turgor pressure (Fig. 6(a)). It further causes the shrinkage in cell size and the decrease of void ratio of cells (Fig. 6(b)), which increases the Young's modulus of cells (Fig. 6(c)). On the other hand, after the water leaves the cells, the volume fraction of intercellular spaces increases (Fig. 6(d)). The expanded intercellular spaces (soft phase) in tissue dominate the process and ultimately soften the apple tissue (Fig. 6(e)).

When the concentration of sucrose becomes high (~30%), the deformation of cells will be much more complex than spherical shrinkage. It is worth noting that the turgor pressure of apple becomes near zero when the concentration of sucrose is over 30% (Fig. 6(a)), which is when the plasmolysis is initiated. And the estimated Young's modulus and Poison ratio are no longer correct. A theoretical model (Nilsson, 1958) had been developed to describe the effect of turgor pressure
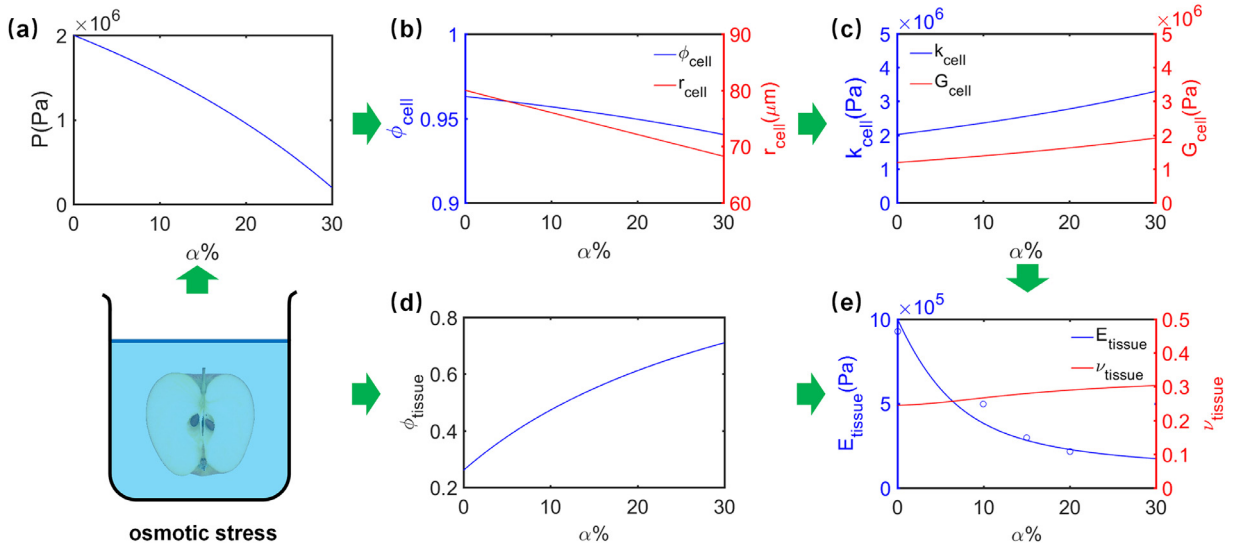
Fig. 6. Effective Young's modulus and Poison ratio of apple tissue under osmotic stress. (a) Change in turgor pressure (P); (b) change in radius (r_{cell}) and volume fraction (ϕ_{cell}) of cytoplasm of cell; (c) change in bulk modulus (k_{cell}) and shear modulus (G_{cell}) of cell; (d) change in volume fraction (ϕ_{tissue}) of intercellular space of tissue; (e) change in Young's modulus (E_{tissue}) and Poisson ratio (υ_{tissue}) of tissue. $\alpha\%$ is the mass fraction of the sucrose solution. The hollow circle represents the experiment results.

and mechanical properties of cell wall on the Young's modulus of tissue, whose results are in agreement with our prediction in tendency. Comparing with the experiment results, the estimated Young's modulus (E_{tissue}) of apple tissue corresponds well.

Interestingly, from the microscopic observation (Fig. 1(a)), the cell size exhibits a gradient of 39–164 μm along the depth of $100 - 1000$ μm near the surface of apple (Fig. S2(a)). Considering the change of cell size in the proposed model, we found that the Young's modulus of apple tissue rises dramatically from 1.0 to 2.3 MPa along the depth (Fig. S2(b)). But the Poison ratio of apple tissue is little influenced by the change of cell size (Fig. S2(b)). The large gradient of Young's modulus resulting from the distribution of cell size could shield the internal apple flesh from external loads. The evolutionary design of apple serves as an inspiration of applications in engineering protection.

4. Conclusion

Based on the observation of fruits microstructure, we developed a cross-scale theoretical model of fruits by combining the van't Hoff theory of osmotic pressure and the self-consistent method. Taking apple as example, we analyzed how the environmental factors (*e.g.*, concentration of solutions or osmotic stress), the microscale structure (*e.g.*, volume fraction of intercellular space, size of cells and thickness of cell wall) and the mechanical properties (*e.g.*, Young's modulus of cell wall and turgor pressure) influence the macroscale mechanical behavior of apple tissue. We found theoretically that increased external osmotic stress changes the osmotic equilibrium, decreases the turgor pressure, shrinks the cells, enlarges the intercellular space and softens the fruit tissue, which agrees with the experimental results. The proposed model can be used to reversely calculate the microscale mechanical properties (*e.g.*, Young's modulus of cell wall) from the macroscale mechanical properties and microstructure of tissue.

Acknowledgements

Supplementary material

Supplementary material associated with this article can be found, in the online version, at doi:10.1016/j.jmps.2019.03.007.

References

Aguilera, J.M., 2005. Why food microstructure? J. Food Eng. 67, 3–11.
Aregawi, W.A., Defraeye, T., Verboven, P., Herremans, E., Roeck, G.D., Nicolai, B.M., 2013. Modeling of coupled water transport and large deformation during dehydration of apple tissue. Food Bioproc. Tech. 6, 1963–1978.
Budiansky, B., 1965. On the elastic moduli of some heterogeneous materials. J. Mech. Phys. Solids 13, 223–227.

Cárdenas-Pérez, S., Chanona-Pérez, J.J., Méndez-Méndez, J.V., Calderón-Domínguez, G., López-Santiago, R., Arzate-Vázquez, I., 2016. Nanoindentation study on apple tissue and isolated cells by atomic force microscopy, image and fractal analysis. Innovat. Food Sci. Emerg. Technol. 34, 234–242.

Cárdenas-Pérez, S., Méndez-Méndez, J.V., Chanona-Pérez, J.J., Zdunek, A., Güemes-Vera, N., Calderón-Domínguez, G., Rodríguez-González, F., 2017. Prediction of the nanomechanical properties of apple tissue during its ripening process from its firmness, color and microstructural parameters. Innovat. Food Sci. Emerg. Technol. 39, 79–87.

Deng, Y., Wu, Y., Li, Y., 2005. Biomechanical properties and texture detection of fruits and vegetables during storage and transportation. Trans. Chin. Soc. Agri. Eng. 21, 1–6.

Dixon, P.G., Muth, J.T., Xiao, X., Skylar-Scott, M.A., Lewis, J.A., Gibson, L.J., 2018. 3D printed structures for modeling the Young's modulus of bamboo parenchyma. Acta Biomater. 68, 90–98.

Eshelby, J.D., 1957. The determination of the elastic field of an ellipsoidal inclusion, and related problems. Proc. R. Soc. Lond. 241, 376–396.

Faisal, T.R., Khalil Abad, E.M., Hristozov, N., Pasini, D., 2010. The impact of tissue morphology, cross-section and turgor pressure on the mechanical properties of the leaf petiole in plants. J. Bionic Eng. 7, S11–S23.

Falk, S., 1958. On the relation between turgor pressure and tissue rigidity 1. Physiol. Plant. 11, 802–817.

Forouzesh, E., Goel, A., Mackenzie, S.A., Turner, J.A., 2013. *In vivo* extraction of Arabidopsis cell turgor pressure using nanoindentation in conjunction with finite element modeling. Plant J. 73, 509.

Franks, P.J., Farquhar, G.D., 2007. The mechanical diversity of stomata and its significance in gas-exchange control. Plant Physiol. 143, 78–87.

Gibson, L.J., 2012. The hierarchical structure and mechanics of plant materials. J. Royal Soc. Interf. 9, 2749–2766.

Hashin, Z., 1962. The elastic moduli of heterogeneous materials. J. Appl. Mech. 29, 143–150.

Hashin, Z., Shtrikman, S., 1962. On some variational principles in anisotropic and nonhomogeneous elasticity. J. Mech. Phys. Solids 10, 335–342.

Hepworth, D.G., Bruce, D.M., 2000. A method of calculating the mechanical properties of nanoscopic plant cell wall components from tissue properties. J. Mater. Sci. 35, 5861–5865.

Hill, R., 1963. Elastic properties of reinforced solids: some theoretical principles. J. Mech. Phys. Solids 11, 357–372.

Hill, R., 1965. A self-consistent mechanics of composite materials. J. Mech. Phys. Solids 13, 213–222.

Hiller, S., Bruce, D.M., Jeronimidis, G., 1996. A micro-penetration technique for mechanical testing of plant cell walls. J. Texture Stud. 27, 559–587.

Horbens, M., Branke, D., Gärtner, R., Voigt, A., Stenger, F., Neinhuis, C., 2015. Multi-scale simulation of plant stem reinforcement by brachysclereids: a case study in apple fruit peduncles. J. Struct. Biol. 192, 116–126.

Hou, C., Liang, Y., Wang, C.G., 2005. Determination of the diffusion coefficient of H_2O in polyacrylonitrile fiber formation. J. Polym. Res. 12, 49–52.

Hu, Y., Suo, Z., 2012. Viscoelasticity and poroelasticity in elastomeric gels. Acta Mech. Solida Sin. 25, 441–458.

Hu, Y., Xin, C., Whitesides, G.M., Vlassak, J.J., Suo, Z., 2011. Indentation of polydimethylsiloxane submerged in organic solvents. J. Mater. Res. 26, 785–795.

Bomben, J.L., K., C.J., 1982. Heat and mass transport in the freezing of apple tissue. J. Food Technol. 17, 615–632.

Jiang, H., Sun, S.X., 2013. Cellular pressure and volume regulation and implications for cell mechanics. Biophys. J. 105, 609–619.

Konstankiewicz, K., Pawlak, K., Zdunek, A., 2001. Influence of structural parameters of potato tuber cells on their mechanical properties. Int. Agrophys. 15, 243–246.

Kroner, E., 1978. Self-consistent scheme and graded disorder in polycrystal elasticity. J. Phy. F Metal Phys. 8, 2261.

Lin, T.T., Pitt, R.E., 2010. Rheology of apple and potato tissue as affected by cell turgor pressure. J. Texture Stud. 17, 291–313.

Liu, G.R., 1997. A step-by-step method of rule-of-mixture of fiber- and particle-reinforced composite materials. Compos. Struct. 40, 313–322.

Markov, P.A., Krachkovsky, N.S., Durnev, E.A., Martinson, E.A., Litvinets, S.G., Popov, S.V., 2017. Mechanical properties, structure, bioadhesion and biocompatibility of pectin hydrogels. J. Biomed. Mater. Res. Part A 105.

Mori, T., Tanaka, K., 1973. Average stress in matrix and average elastic energy of materials with misfitting inclusions. Acta Metall. 21, 571–574.

Nemat-Nasser, S., Hori, M., 1993. Micromechanics: overall properties of heterogeneous materials. Appl. Math. Mech. 37, 354–355.

Nilsson, 1958. On the relation between turgor pressure and tissue rigidity2. Physiol. Plant. 11, 818–837.

Oey, M.L., Vanstreels, E., De Baerdemaeker, J., Tijskens, E., Ramon, H., Hertog, M.L.A.T.M., Nicolaï, B., 2007. Effect of turgor on micromechanical and structural properties of apple tissue: a quantitative analysis. Postharvest Biol. Technol. 44, 240–247.

Ordazortiz, J.J., Marcus, S.E., Knox, J.P., 2009. Cell wall microstructure analysis implicates hemicellulose polysaccharides in cell adhesion in tomato fruit pericarp parenchyma. Mol. Plant 2, 910–921.

Piotrowski, D., Golos, A., Grzegory, P., 2014. Shrinkage and mechanical properties of defrosted strawberries dried by convective. Vacuum Convective-vacuum Methods.

Singh, F., Katiyar, V.K., Singh, B.P., 2013. A new strain energy function to characterize apple and potato tissues. J. Food Eng. 118, 178–187.

Singh, F., Katiyar, V.K., Singh, B.P., 2014. Analytical study of turgor pressure in apple and potato tissues. Postharvest Biol. Technol. 89, 44–48.

Wang, C.X., Wang, L., Thomas, C.R., 2004. Modelling the mechanical properties of single suspension-cultured tomato cells. Ann. Bot. (Lond.) 93, 443–453.

Wang, R., Li, W., Ji, B., Fang, D., 2017. Fracture strength of the particulate-reinforced ultra-high temperature ceramics based on a temperature dependent fracture toughness model. J. Mech. Phys. Solids 107, 365–378.

Wei, C., Lintilhac, P.M., 2007. Loss of stability: a new look at the physics of cell wall behavior during plant cell growth. Plant Physiol. 145, 763–772.

Zhu, H.X., Melrose, J.R., 2003. A mechanics model for the compression of plant and vegetative tissues. J. Theor. Biol. 221, 89–101.